Assessing airborne infection risk through a model of airflow evacuation and recirculation dynamics

Alan Kabanshi*, *Harald* Andersson, *Mikael* Sundberg, *Dario* Senkic and *Mats* Sandberg

Department of Building Engineering, Energy Systems and Sustainability Science, University of Gävle, 801 76 Gävle, Sweden

Abstract. In a ventilated room, the indoor airflows are complicated but can generally be defined by an internal recirculating airflow generated by flooding of ventilation air. This concept categorizes the internal room flow (air and contaminants) as consist of two populations: One leaving the room and the other recirculating. The one recirculating is spreading the contaminants while the one leaving is evacuating the contaminants, which are quantified by the transfer probability between the source and other locations in the room and by purging flow rate, respectively. This concept accounts for spatial and temporal aspects in risk of airborne infection transmission. The current paper proposes and discusses a revised risk infection model based on this concept and has demonstrated applicability of the model with a test measurement setup with both mixing and displacement ventilation systems. The results emphasize the importance of considering both spatial and temporal factors in assessing airborne infection risks. It underscores the need for dynamic models like the proposed revised Wells-Riley model to provide a more accurate representation of infection risks in various indoor environments. Additionally, it discusses the necessity for longer measurement periods to fully understand the evolving nature of these risks.

1 Introduction

In ventilation practices, it is standard to filter and condition outdoor air during intake and to seal the building effectively to limit unintended airflows [1]. The approach primarily focusses to dilute pollutants generated indoors using the incoming airflow [2]. However, this approach is insufficient for preventing the spread of airborne infections, necessitating significantly higher ventilation rates. Yu et al. [3] suggested increasing ventilation air change rate to at least 9/h to effectively reduce infection risk. Jiang et al. [4] analysed the 2002 severe acute respiratory syndrome virus (SARS) outbreak and concluded that ventilation rates should be high enough to replace air exhaled by an infected individual with clean air by a factor of 10000. Since airborne infections predominantly originate and transmit indoors from infectious occupants [5], existing ventilation strategies are limited and recommended operational flowrates are unrealistic for ordinary buildings. Thus, recommendations like social distancing and self-isolation may be inadequate for indoor infection control.

Current ventilation systems in buildings are not designed with airborne infection protection in mind. The airflow dynamics within buildings can therefore facilitate the spread of infections, especially in poorly ventilated spaces where the risk of contaminant flooding is high. In typical buildings, ventilation dynamics can inadvertently aid in spreading infections. This risk escalates in systems that recycle part of the exhaust air without use of high-quality filtration, which is both costly and maintenance-intensive [6]. Otherwise, the spread is caused by indoor airflows, which can be described as both diluting the concentration of infectious agents and spreading infectious agents [7]. For instance, even in well managed cases of self-isolating, air exchange through doorways can serve as a transmission pathway. The flowrate in doorways is normally much larger than the exhaust ventilation flowrate [8], and door movements, i.e., opening and closing, generates large air volume transfer by "door swing pumping" [2].

Moreover, prevalent ventilation designs often involve individual air supply units in rooms but share a common exhaust unit, usually located in bathrooms or/and kitchens for residential buildings. This results in air mixing from various areas and rooms before expulsion from the building. Indoor airflow dynamics are characterized by interaction of buoyancy driven flows combined with the ventilation system, leading to complex indoor airflow motions involving air transfer between regions and recirculation, aspects often oversimplified or ignored in current ventilation practices and airborne infection risk models. Zhang and Lin [9] critiqued the Wells-Riley model for being overly simplistic and not accurately reflecting the dynamic and heterogeneous nature of indoor environments. They argued that this could lead to underestimating or overestimating infection risks and adoption of inappropriate mitigation strategies. Similarly, they point out that the modified Wells-Riley model (rebreathed-fraction model) by Rudnick and Milton [10] is also limited due to its assumption of a uniformly mixed

* Corresponding author: alan.kabanshi@hig.se

environment and thus lacks spatial resolution. In response, Zhang and Lin [9] introduced a dilution-based airborne infection risk model, offering better spatial and temporal resolution. However, it does not fully address the effects of air recirculation and contaminant evacuation. Besides, the removal of the number of infectious (emission sources) will limit its application as the contaminant generation rate will also be limited consequently also the effect or recirculation. We propose considering three key factors in assessing risk of infection as an aspect of airflow and contaminant distribution in indoor settings: the likelihood of contaminant transfer from the source to the target, the impact of indoor air recirculation, and the contaminant evacuation efficiency at the target location [6, 11].

2 Proposed Modified Wells-Riley Model

The risk of being infected model assumes that in the building or room there is more than one occupant and that at least one is infected. If they are in the same room, they are regarded as being in different zones and the size of the zone can vary but it can for example correspond to micro-environment around human body or the breathing domain area, which additionally can be defined by the social distancing recommendation. If they are in different rooms the zone is equal to the room (compartment). The compartments or zones interact with each by exchange of airflows either through forced mechanisms (ventilation driving flow) or driven by the temperature differences between them or both, which earlier was argued that it develops complicated indoor airflow interaction dynamics. The basic mathematical unit in a multiple zone model is the transfer probability matrix. [12] shows how to use the multiple zone representation of a building for predicting the air quality related parameters as purging flow rate ventilating the compartments. The proposed modified model takes this approach based on the purging flowrate characterizing the dilution capacity and the visitation frequency concept, a new metric for characterizing the spread of contaminants within a room or building [11]. This concept has been developed in several papers [6], [13–15].

Herein, we propose a revised risk infection model that is based on the classical Wells-Riley model [16], Eq. (1), that defines the probability of infection (*Pi*) as a function of *I* the number of infectors; *p* the pulmonary ventilation rate (m^3/h) i.e., the rate at which a person inhales air, *q* the quantum generation rate (quanta/h) or the rate at which infectious aerosols are produced by an infectious person, Q_v the room ventilation flowrate (m^3/h) and *t* the time length of the exposure period (h).

$$Pi = 1 - e^{-(\frac{Iq}{Qv}pt)} \quad (1)$$

where the ratio Iq/Q_v represents the inhalation dose that the susceptible occupants are exposed to.

Despite its limitations on the lack of spatial accountability (assumes infectious aerosols are evenly distributed), the Wells-Riley model provides a useful framework for understanding and mitigating airborne infection risks. E.g., (1) Dilution of infectious agents reduces the probability of infection, and (2) the significance of exposure time and the control of sources of infection or infectious agent evacuation.

We propose, in Eq. 2, a revised probability of infection risk (P_r) that is based on the airflow interactions and characteristics in a domain within the room Fig. 1. The model complements the Wells-Riley model by introducing the transfer probability (P_t) and replacing the ventilation flowrate with the local purging flowrate (Q_p), thus accounting for the actual movement of air and contaminants within and between zones.

$$P_r = 1 - e^{-(\frac{P_t Iq}{Qp}pt)} \quad (2)$$

Where the ratio P_tIq/Q_p represents the inhalation dose for the susceptible occupants. Under perfect mixing conditions and applying conservation of mass, the transfer probability is unity, and the local purging flowrate is equal to the room ventilation flowrate. Therefore, the proposed model (Eq. 2) reduces to the Wells-Riley model (Eq. 1).

2.1 Transient Analysis of Contaminant Concentration and Purging Flowrate in a Local Zone.

Figure 1 demonstrates the interaction of flows at a local domain in a room, which is a representation of a zone (target domain) in a room. For the target domain with volume (*V,* m^3) the inflow rates, defined by Q_{in} (m^3/s) as incoming flowrate from outside the domain (transferring new particles and contaminants) and Q_r (m^3/s) as recirculating flowrate (returning old particles and contaminants that once was in the domain) is equal to Q_p the evacuation flowrate (m^3/s) that takes away particles and contaminants to never return to the domain [7]. Evacuation flowrate is defined as the purging flowrate which is an index of ventilation efficiency that controls contaminant removal in a local domain [6, 17].

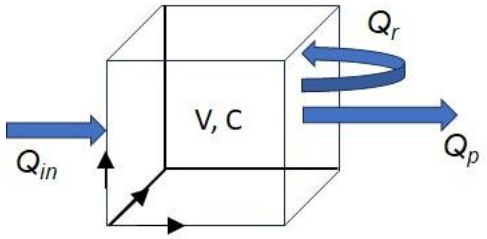

Fig. 1. Airflow interaction characteristics for a defined zone or domain in a room.

To derive a time-dependent equation for the concentration of contaminants in the domain, we can set up a balance equation considering the mass of contaminants entering, leaving, and being recirculated to the domain which is assumed to have a homogeneous contaminant concetration C.

If *C(t)* is the concentration of contaminants within the domain at time *t*, and *Cd* is the concentration of contaminants in the incoming flow directly from the

source. The rate of change of the mass of contaminants within the domain is then given by the rate at which contaminants are brought into the domain by the incoming flow and recirculating flow, minus the rate at which contaminants are purged from the domain. Assuming quasi-steady state, the rate of change of the mass of contaminants is defined by the equation.

$$\frac{d(CV)}{dt} = Q_{in}C_d(t) + rQ_rC(t) - Q_pC(t) \quad (3)$$

Where r is the probability to return, C_d is the direct transfer from the source in another region in the room (through Q_{in}) and r as the probability of contaminants leaving the domain and returning. The equation can be simplified to

$$\frac{dC}{dt} = \frac{1}{V}[Q_{in}C_d(t) + rQ_rC(t) - Q_pC(t)] \quad (4)$$

we should treat each term individually to reflect that each flow contributes differently to the contaminant concentration within the domain, thus:

$$\frac{dC}{dt} = \frac{Q_{in}}{V}C_d(t) + \frac{Q_r}{V}rC(t) - \frac{Q_p}{V}C(t) \quad (5)$$

This equation assumes the concentration varies with time while the interacting flowrates are under steady state (which was the observed tendency in the preliminary longer measurements). In this case we are also assuming the probability to return is constant. If the conditions in the room are transient, then all factors are time dependent (usually the case just after occupancy before reaching steady state or when there is a disturbance due to movements or a huge shift on airflow patterns in the room). And thus:

$$\frac{dC}{dt} = \frac{Q_{in}(t)}{V}C_d(t) + \frac{Q_r(t)}{V}r(t)C(t) - \frac{Q_p(t)}{V}C(t) \quad (6)$$

In a case we don't know or can't determine the probability to return, we can modify the second term for returning characteristics by replacing the term $[\frac{Q_r(t)}{V}r(t)C(t)]$ with $[\frac{Q_r(t)}{V}C_r(t)]$, where C_r is the contaminant concetration returning back to the region. Thus the equation can be represented as:

$$\frac{dC}{dt} = \frac{Q_{in}(t)}{V}C_d(t) + \frac{Q_r(t)}{V}C_r(t) - \frac{Q_p(t)}{V}C(t) \quad (7)$$

This defines the rate of change of the mass of contaminants within the domain given by the rate at which contaminants are brought into the domain by the incoming flow and recirculating flow, while accounting for the rate at which contaminants are evacuated from the domain. This can be simplified as a time dependent inflow flux (F_{in}) and as such the contribution of contaminants of each component to the concetration in a domain will vary with time and indoor environmental conditions. E.g., direct transfer will dominate concetration contribution in the early occupancy time, but after a while (assuming a steady-state dynamics) the contaminant contribution is determined by superimposing the dominating air flowrate of the target domain. Recirculation is determined by the visitation frequency, where a particle enters the local domain for the first time, is transported to the outside, and then returns to the local domain because of air distribution in the room [6, 11]. The internal airflows because of occupant behaviour, internal heat sources or solar insolation will influence recirculation characteristics. Applying the concept of the quantum, the transfer probability can then be presented as

$$P_t = \frac{F_{in}}{Iq} \quad (8)$$

The revised model, with its focus on airflow dynamics and spatial differentiation, offers a more nuanced and a better representation for the complex airflow distribution in indoor environments.

To determine the purging flowrate, Figure 2 shows the domain with volume V and having an internal contaminant generation source with the dosing flowrate Q_d and dosing contaminant concetration C_d. The incoming flowrate Q_{in} carries contaminant concetration C_{in} which accounts for both the recirculation and non-recirculation flow of contaminants onto the local domain.

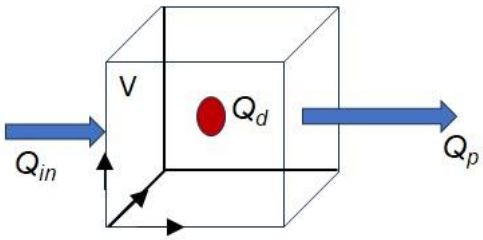

Fig. 2. Airflow interaction characterising empirical determination of the purging flowrate.

Considering mass balance, we derive the purging flowrate as a time dependent function:

$$Q_p(t)C_o(t) = Q_{in}(t)C_{in}(t) + Q_d(t)C_d(t) \quad (9)$$

thus,

$$Q_p(t) = \frac{Q_{in}(t)C_{in}(t)+Q_d(t)C_d(t)}{C_o(t)} \quad (10)$$

If the domain boundary is assumed to be a contaminant concetration sensor, then the measured concetration C_m can be assumed to be an average concetration of both the incoming and outgoing concetration in the globe. Then, since the mass balance equation includes C_{in}, C_d and C_o, then C_m can be an intermediate variable that helps to determine C_o.

$$C_m(t) = \frac{C_{in}(t)+C_o(t)}{2} \quad (11)$$

$$C_o(t) = 2C_m(t) - C_{in}(t) \quad (12)$$

This approach holds true if there is continuous perfect mixing with the globe and there is no accumulation or complete depletion of contaminants within the domain overtime. Thus, assuming steady state conditions in the globe and perfect mixing, we can expand equation 10 to:

$$Q_p(t) = \frac{Q_{in}(t)C_{in}(t)+Q_d(t)C_d(t)}{2C_m(t)- C_{in}(t)} \quad (13)$$

Practically, $Q_{in}(t)C_{in}(t)$ will be much less than $Q_d(t)C_d(t)$ thus can be neglected, and $C_{in}(t)$ is very close to the room average concetration.

The current analysis of the purging flowrate estimates the air distributions capacity to evacuate contaminants generated in a zone. One can assume that for any air distribution system the contaminant evacuation capacity will be the same whether the source is local or has been transported into the zone from a different zone, since the effect of airflow characteristics acting on the domain are the same.

3 Demonstration of applicability of the revised model

Spatial differentiation in indoor environments refers to the heterogeneity in environmental conditions such as air quality, temperature, and airflow patterns across various segments or zones of a given space. A comprehensive analysis of these airflow dynamics is crucial for understanding the mechanisms of aerosol propagation and accumulation, which in turn, are pivotal for devising effective strategies to mitigate and lower the risks of infection transmission. Within this framework, our study delves into the spatial and temporal disparities in the efficacy of mixing and displacement ventilation systems, examining these disparities through the prism of transfer probability and their ramifications on the infection risk model we propose.

To facilitate our investigation, experimental measurements were conducted in a climate chamber at The University of Gävle, Sweden. The room was modelled as a mock-up study room with dimensions of 4 meters in length, 4 meters in width, and a ceiling height of 2.5 meters. This chamber was outfitted with two distinct ventilation systems, each independently controlled to enable a comparative analysis of displacement ventilation (DV) and mixing ventilation (MV) strategies. As shown Figure 3, the setup included four human thermal manikins, engineered to simulate the thermal output of occupants by generating 100 Watts of heat each. The contamination source is designated red, whereas the other manikins symbolize individuals susceptible to infection. The ventilation systems operated at an airflow rate of 130 m^3/h and with the supply air temperature maintained at 18°C.

Carbon dioxide (CO_2) served as the tracer gas for evaluating both the transfer probability of the contaminant from the source to susceptible zones, and the local ventilation conditions were assessed by purging flowrates. The strategic positioning of the measurements at a height of 1.1 meters corresponded to the typical mouth region of an occupant, thus representing the effective zone of inhalation and exhalation. The measurement device, a prototype globe developed in-house, was engineered to ascertain the average tracer concentration within this specified volume. The globe consisted of four polyvinyl chloride (PVC) tubes, each with an exterior diameter of 4 mm and an interior diameter of 2.5 mm, organized in a circular array and interconnected at their apex (shown on the top right in Fig. 3). These tubes, extending 600 mm in length, were perforated with 30 apertures, each 20 mm apart and 0.8 mm in diameter. At the globe's core, a doser discharged CO_2 during the purging flowrate assessments through a nozzle measuring 0.8 mm in diameter, directing a jet of a CO2 and air mixture onto a 40 mm diameter circular plate. It is postulated that the CO2 disperses and mixes homogeneously throughout the globe's volume, which is presumed to represent the effective breathing volume for the purposes of this study. For illustrative clarity, the present analysis adopts the globe's diameter of 191 mm, which encompasses a breathing volume of 3.6 litres (0.0036 m^3).

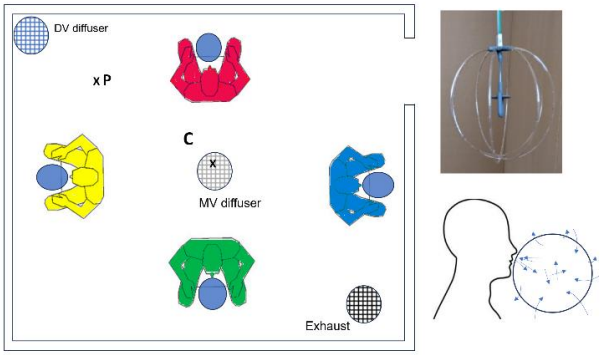

Fig. 3. Measurement setup, the measurement globe, and the domain of interest (breathing region).

The temperature distribution within the room, as depicted in Figure 4, illustrates the distinctive characteristics of the thermal conditions attributable to each ventilation strategy.

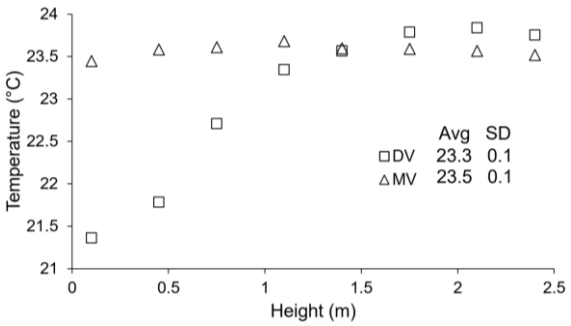

Fig. 4. Temperature distribution in the room.
Note: Average (Avg) room temperature at 1.1 m

Specifically, the buoyancy-driven profile associated with displacement ventilation epitomizes the stratification inherent to such systems, whereas the thermal dispersion under mixing ventilation is indicative of effective homogenization of air temperatures. Quantitatively, the mean surface temperature and its standard deviation (SD) were recorded at 23.5 °C and

0.45 °C for displacement ventilation, and 24.1°C and 0.1°C for mixing ventilation, respectively. These measurements underscore the differential thermal dynamics and consequently gives a picture of the associated airflow patterns facilitated by the respective ventilation approaches.

During the experimental measurements, a controlled admixture of 0.033 m³/s of compressed air with 0.00167 m³/s of CO_2, culminating in a concentration of approximately 48,039 ppm, was introduced into the breathing zone of a designated red manikin. Concurrently, concentration measurements were systematically done at analogous positions relative to the other manikins. The measurements were carried out using the novel in-house developed tracer gas system, FAST-AIR (Fast Analytic Systems for Tracer-gas Assessment in Indoor Research), characterized by a sampling interval and rate of one second and a measurement precision of ±5 ppm. For an exhaustive description of this system, refer to [18].

This study presents initial observations over a duration of 100 minutes of occupancy for each experimental setup. As illustrated in Figure 5, the concentrations peaking at the injection site and quickly attains a state of equilibrium, albeit with noticeable variations especially in the mixing ventilation. Speculatively, we can attribute this behaviour to turbulent characteristics of airflow in the breathing zone under mixing ventilation. On the other hand, displacement ventilation system has a stratified flow which is damping out the turbulence.

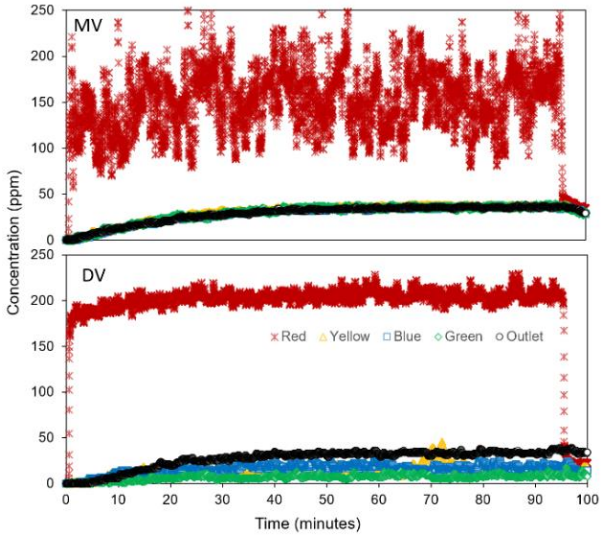

Fig. 5. CO_2 concentrations at the source (Red) and target domains including the exhaust (Black).

A discernible lag in tracer dispersion from the point of introduction to designated target zones was observed, with no differences between the systems. A closer look at dispersion pattern of the tracer gas at different target regions demonstrate variability as seen in Figure 6. Notably, the dispersion under mixing ventilation exhibited a greater degree of uniformity, in contrast to the spatial and temporal heterogeneity observed under displacement ventilation, aligning with findings from previous studies [9], [19]. This delineates the distinct influence of ventilation strategies on the dynamics of tracer gas distribution within indoor environments, highlighting both spatial and temporal disparities.

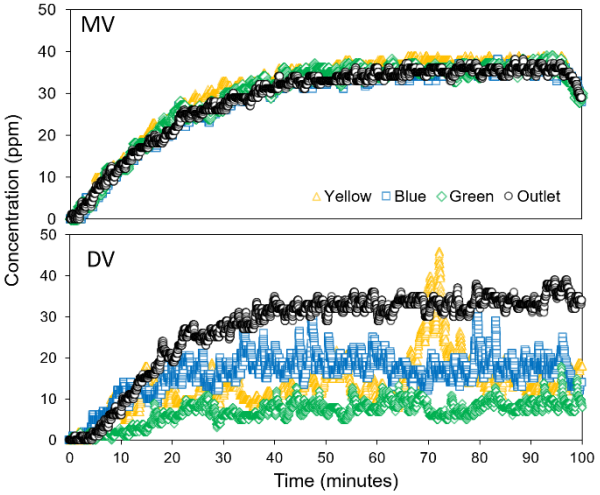

Fig. 6. CO_2 concentrations at different target domains with time.

The concept of transfer probability, as delineated in Figure 7, mirrors the concentration profiles documented in Figure 6, presenting an intriguing correlation between these two phenomena. Within the context of mixing ventilation, the congruence of measurements at targeted locations signifies a negligible spatial variation, albeit with discernible temporal fluctuations. This contrasts sharply with the scenario under displacement ventilation, where measurements unveil pronounced disparities across both spatial and temporal dimensions, thus underscoring the divergent airflow dynamics intrinsic to each ventilation modality.

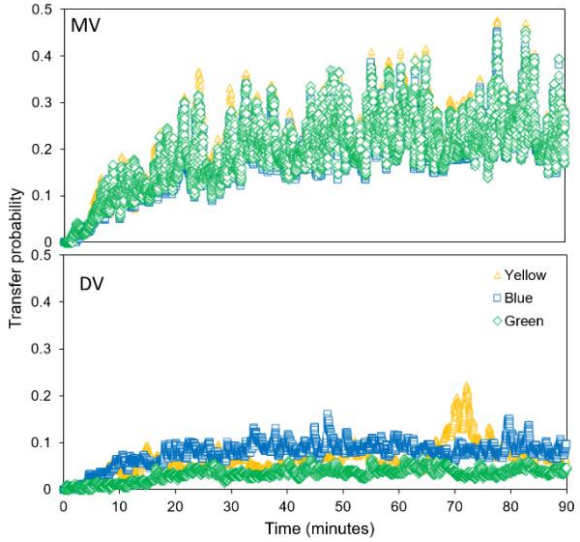

Fig. 7. Transfer probability as a function of time.

The observation suggests that in environments characterized by thorough mixing, the exposure to indoor contaminants is relatively homogenous across different spatial locations, albeit subject to temporal variations that arise from the specific attributes of the airflow patterns. Conversely, in settings governed by displacement ventilation, the exposure to contaminants is modulated by spatial positioning engendering a more stochastic (or randomly determined) exposure pattern. The temporal dynamics are due to the unstable and are

swaying of thermal plumes, which are the driving flows in displacement ventilation. This dichotomy accentuates the criticality of integrating both spatial and temporal considerations into the assessment of indoor air quality and the quantification of exposure risks.

The purging flow rate plays a pivotal role in evaluating the efficacy of contaminant removal from a room and within zones in an indoor environment. Figure 8 presents the purging flow rate as a dynamic parameter over time for each domain, underscoring its criticality in assessing the effectiveness of contaminant evacuation. It is important to acknowledge that the measurements pertinent to the determination of the purging flow rate were executed independent to the concentration measurements for each target location, necessitated by the requirement for localized dosing. This approach ensures that the data accurately reflects the contaminant evacuation capacity at each specific location although differences due to temporal resolution may arise.

Employing Equation 13 for the computation of the purging flowrate unveils significant spatial and temporal heterogeneities in its effectiveness. As shown in the boxplots, spatial disparities are particularly accentuated under displacement ventilation than mixing ventilation, while scatterplot shows that temporal disparities are frequent under mixing ventilation. This can be attributed to turbulence and an indication of increases recirculation of airflow in the target domains under mixing ventilation. For instance, the domain designated as 'Blue' exhibits higher values and displays the greatest degree of variability, and 'Yellow' is characterized by the lower value and least variability (see boxplots). Mixing ventilation suggests a more homogeneous air change efficacy, albeit with more variability during the measurement period. Under displacement ventilation, this analysis indicates that the proficiency of contaminant extraction is not uniformly distributed across the room's various domains. This variability is clearly marked, signalling that certain zones may exhibit suboptimal contaminant removal capabilities, e.g., 'Yellow' in comparison to 'Blue'.

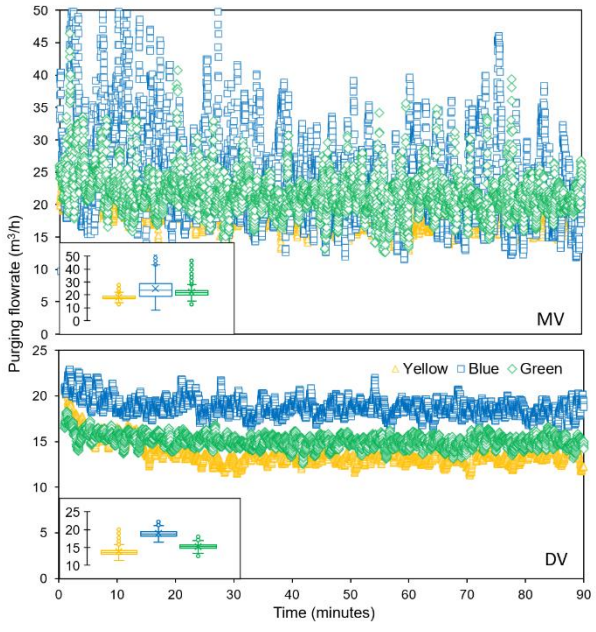

Fig. 8. Purging flowrate as a function of time.

An interesting observation is that the target domain purging flowrates are lower under displacement ventilation than mixing ventilation, which contrast studies using concepts of contaminant removal efficiency, mean age of air or local air change efficiency [20-22]. We think that the results are lower under displacement ventilation because thermal plumes are the driving flows in stratified environments and the purging flowrate in the breathing domain will be influenced by the strength of the plumes and other interacting internal airflows. Further studies needed to verify the results and substantiate the given explanation. Overall, the effectiveness of contaminant purging is observed to evolve spatially and temporally, highlighting the non-static nature of the purging flowrate which undergoes fluctuations over time.

The spatial and temporal disparities observed in the indoor environmental conditions herein indicate that the risk of infection will vary across different areas and evolve over time. Figure 8 illustrates these variations by employing Equation 2 a modified version of the Wells-Riley equation, which integrates time-dependent transfer probabilities and purging flow rates to ascertain the infection risk. The current study makes calculations of the infection risk by adopting a quantum generation rate of 142 quanta/h, indicative of the emission rate from a COVID-19 infected individual, as delineated by Zhang and Lin et al. [9]. Additionally, it incorporates a pulmonary ventilation rate of 0.52 m³/h for sedentary activities, based on Buonanno et al. [23].

The analysis reveals that the risk of infection at designated target domains escalates with increased occupancy duration. Notably, under mixing ventilation, the infection risk ascends more precipitously compared to displacement ventilation, a trend that aligns with the observed higher purging flow rates under displacement ventilation. This suggests that displacement ventilation might present a more advantageous scenario in mitigating infection risk. In both ventilation systems, the spatial and temporal dynamics significantly modulate the infection risk.

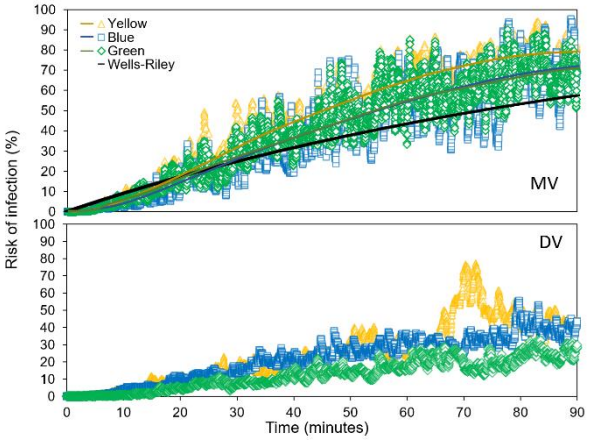

Fig. 9. Airborne infection risks at different target positions as a function of time.

Furthermore, a comparative analysis with the original Wells-Riley model within mixing ventilation framework highlighted that the conventional model tends to overestimate the infection risk during the initial

20 minutes of exposure. Conversely, the revised model, accounting for spatial and temporal variations, projects a more gradual escalation of risk. Over prolonged periods, the traditional Wells-Riley model is posited to underestimate the risk, particularly for extended occupancy durations. This observation underscores the necessity for longitudinal studies to accurately capture the dynamic nature of infection risk, emphasizing the critical role of both spatial and temporal factors in shaping the indoor transmission dynamics of airborne pathogens.

Such insights add emphasis on the necessity for a nuanced approach in the evaluation of ventilation strategies, where the aim is not only to ensure effective dispersal of airborne contaminants but also to mitigate exposure risks in a manner that is informed by the complex interplay between airflow dynamics, spatial distribution, and temporal variability. This comprehensive understanding is pivotal for the development of more effective indoor air quality management practices and the formulation of guidelines that are attuned to the multifaceted nature of exposure risks within indoor environments.

4 Discussion and conclusion

The enhanced infection risk model introduced in this discourse significantly advances our understanding of airborne disease transmission in indoor spaces by incorporating spatial and temporal dimensions of indoor air distribution. This model distinguishes itself by accounting for the dynamics of contaminant transfer from the source to susceptible targets, the implications of indoor air recirculation patterns, and the capacity for contaminant evacuation at specific locations. Such parameters are inherently time-variable, adjusting to the instantaneous changes in airflow dynamics, which in turn modulate the risk of infection. This methodological approach provides a nuanced depiction of the complex interplay between airflow patterns and objective environmental conditions in influencing viral transmission, offering a more precise reflection of the multifaceted nature of real-world indoor environments.

The results from applying this model have profound implications for the management of indoor environmental quality. The analysis suggests that mixing ventilation systems, while promoting a more consistent environmental condition, may exhibit higher rates of contaminant transfer, increased recirculation possibly creating zones of stagnant air that heighten infection risk. Conversely, displacement ventilation systems may achieve higher contaminant removal efficiency at certain times but also suffer from periods of diminished effectiveness on the purging flowrate.

Recirculation is caused by flooding and flooding happens because the evacuation capacity of the ventilation system is less than the flow rate generated internally within the room. In mixing ventilation, the whole room is a recirculation zone but in displacement ventilation only a fraction of a room is a recirculation zone (the region above the inversion point). Subsequently the recirculation is less in displacement ventilation than in mixing ventilation. These insights underscore the importance of meticulous ventilation system design and management to ensure optimal air quality throughout indoor spaces.

Nevertheless, the complexity and data-intensive nature of this refined model pose certain challenges to its widespread implementation. The accuracy of the model depends on detailed data collection, particularly for parameters like transfer probability and purging flow rate, which are crucial yet currently under refinement. The need to incorporate indoor air recirculation into the transfer probability calculations introduces additional complexity, as current methodologies may not adequately capture this aspect. Hence, the development of new ventilation indices that comprehensively account for contaminant transfer, recirculation, and evacuation is imperative.

While the Wells-Riley model has served as a foundational tool in assessing airborne infection risk due to its simplicity and practicality, it falls short in capturing the dynamic and heterogeneous nature of indoor airflows, potentially leading to overestimation or under estimation of the infection risk as shown herein, consequently will lead to ineffective or misinformed mitigation strategies.

Future directions for enhancing this model include simplifying its application to increase accessibility for real-world applications, integrating it with real-time indoor environment monitoring systems to leverage advancements in sensor technology, and conducting extensive validation studies across diverse indoor settings to affirm its reliability and relevance. Additionally, broadening the model to encompass other transmission pathways, such as fomite transmission, could provide a more holistic view of infection risks.

In summation, this study presents a revised Wells-Riley model that adeptly addresses the spatial and temporal complexities of indoor air distribution, demonstrating its applicability across environments characterized by both homogeneous and heterogeneous conditions. Despite challenges related to its complexity and the demands for detailed data, the model's emphasis on spatial and temporal differentiation is vital for accurately assessing airborne infection risks in dynamic indoor settings. With future enhancements and technological integration, this model promises to become an essential resource for public health officials and building design professionals, facilitating the development of strategies that effectively mitigate airborne disease transmission.

Acknowledgement

This work is partly supported by FORMAS (Dnr: 2021-01606) under the project “Ventilation as a strategy to reduce indoor transmission of airborne diseases: Development of new strategies and a risk assessment model”.

References

1. A. Fernstrom, M. Goldblatt. J. Pathog **2013**, (2013).
2. D.W. Etheridge, M. Sandberg. *Building Ventilation: Theory and Measurement*, ISBN 9780471960874. (John Wiley & Sons: Chichester 1996)
3. H.C. Yu, K.W. Mui, L.T. Wong, H.S. Chu. Indoor Built Environ **26**, 514–527 (2017).
4. Y. Jiang, B. Zhao, X. Li, X. Yang, Z. Zhang, Y. Zhang. *Investigating a Safe Ventilation Rate for the Prevention of Indoor SARS Transmission: An Attempt Based on a Simulation Approach*, in Proceedings of the Building Simulation **2**, 281–289, (2009).
5. L. Dietz, P.F. Horve, D.A. Coil, M. Fretz, J.A. Eisen, K. Van Den Wymelenberg. Msystems **5**, e00245-20 (2019).
6. E. Lim, M. Sandberg, K. Ito. Indoor Air **31**, 1267–1280 (2021).
7. M. Sandberg, M. Front. Built Environ **7**, (2022).
8. C. Blomqvist, PhD diss., KTH, (2009).
9. S. Zhang, Z. Lin. Build Environ **194**, 107674, (2021).
10. S.N. Rudnick, D.K. Milton. Indoor Air **13**, 237–245 (2003).
11. M. Sandberg, A. Kabanshi, H. Wigö. Indoor Built Environ **29**, (2020). doi:10.1177/1420326X19837340.
12. M. Sandberg, M. Build. Environ **19**, 221–233 (1984).
13. E. Lim, K. Ito, M. Sandberg. Build. Environ **61**, 45–56 (2013).
14. E. Lim, K. Ito, K.M. Sandberg. Build Environ **79**, 78–89 (2014).
15. J. Chung, E. Lim, M. Sandberg, K. Ito. Build Environ **125,** 67–76 (2017).
16. W.F. Wells. *Airborne Contagion and Air Hygiene: An Ecological Study of Droplet Infections*; Commonwealth Fund (1955).
17. M. Sandberg. *Ventilation Effectiveness and Purging Flow Rate-a Review*. Int. Symp. Room Air Convect. Vent. Eff. (1992).
18. H. Andersson, M. Sundberg, D. Senkic, M. Sandberg, A. Kabanshi. *FAST-AIR: Fast Analytic Systems for Tracer-Gas Assessment in Indoor Research - Development and Testing of CO2 Tracer-Gas System,* in proceedings of RoomVent Conf. 22nd-25th April. Stockholm, Sweden (2024).
19. W. Su, B. Yang, A. Melikov, C. Liang, Y. Lu, F. Wang, A. Li, Z. Lin, X. Li, G. Cao. Build. Environ **207**, 108555 (2022).
20. B. Yang, Z. Lin, A. Li. Trends Civ Eng Mater Sc, 1–2 (2018).
21. A. Kabanshi, H. Wigö, M. Sandberg. Build Environ **95**, 240–250 (2016).
22. G. Cao, H. Awbi, R. Yao, Y. Fan, K. Siren, R. Kosonen, J. Zhang. Build. Environ **73**, 171–186 (2014).
23. G. Buonanno,L. Stabile, L. Morawska. Environ Int **141**, 105794 (2020).